

Pivotal Role of Snow Deposition and Melting Driving Fluxes of Polycyclic Aromatic Hydrocarbons at Coastal Livingston Island (Antarctica)

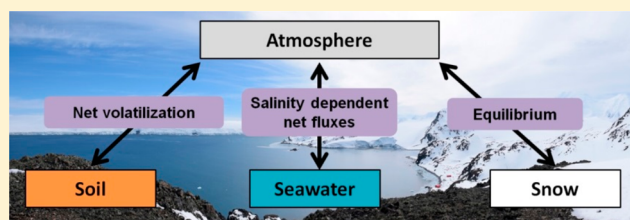
Paulo Casal,[†] Ana Cabrerizo,[†] Maria Vila-Costa,[†] Mariana Pizarro,[†] Begoña Jiménez,[‡] and Jordi Dachs^{*,†}

[†]Institute of Environmental Assessment and Water Research, Spanish National Research Council (IDAEA-CSIC), Jordi Girona 18-26, Barcelona, Catalonia 08034, Spain

[‡]Department of Instrumental Analysis and Environmental Chemistry, Institute of Organic Chemistry, Spanish National Research Council (IQOG-CSIC), Madrid 28006, Spain

Supporting Information

ABSTRACT: The atmosphere–land–ocean dynamics of semivolatile organic compounds in polar regions is poorly understood, also for the abundant and ubiquitous polycyclic aromatic hydrocarbons (PAHs). We report the concentrations and fluxes of PAHs in a polar coastal ecosystem (Livingston Island, Antarctica). From late spring (December 2014) to late summer (February 2015), we sampled air, snow, coastal seawater, plankton, and the fugacity in soils and snow. The concentrations of PAHs in seawater were low but increased during the austral summer. The PAH concentrations in snow were significantly higher than in coastal seawater. Soil–air fugacity ratios showed a net volatilization of PAH when soils were covered with lichens, and close to air–soil equilibrium for bare soils. Concentrations in surface snow were also close to equilibrium with atmospheric PAHs. Conversely, there was a net diffusive deposition of PAHs to coastal seawater during late spring, but a net volatilization from seawater during late summer. Volatilization fluxes were correlated with seawater temperature and salinity, consistent with a key role of snowmelt to the fluxes and dissolved phase concentrations during the austral summer. The comprehensive assessment provided here shows that the fugacity amplification in snow is transferred to soils and coastal seawater supporting PAH concentrations and fluxes.



INTRODUCTION

Polycyclic aromatic hydrocarbons (PAHs) are semivolatile organic compounds (SVOCs) mainly generated from the incomplete combustion of fossil fuels and organic matter, being ubiquitously found in the global environment.^{1–3} PAHs are under international regulation by the United Nations Economic Commission for Europe Convention on Long-Range Transboundary Air Pollution, due to their widely reported harmful and carcinogenic effects.^{4,5} PAHs can be found even in remote regions such as Antarctica^{1,2} due to their susceptibility for long-range atmospheric transport (LRAT) coupled with deposition favored by cold trapping⁶ and air–seawater disequilibrium in the open ocean.² Additionally, tourism and research stations have been suggested as a significant local source of PAHs, especially in Antarctic soils.^{7,8}

Nevertheless, there are few studies on the occurrence of PAHs in Antarctic snow, soils, air, seawater, sediments, and biota.^{1,2,9–14} Notwithstanding, the Antarctic region is still understudied in comparison to other remote areas such as the Arctic.¹⁵ The dynamic coupled fluxes between the different Antarctic compartments are poorly understood as their assessment require a multimedia approach comprising the analysis of different environmental matrices, and the assess-

ment of fluxes among air, water, snow, and soils. Conversely, previous Antarctic SVOCs assessments tended to focus on individual compartments or processes. The few multicompartamental works on PAHs include the determination of volatilization of 3–4-ring PAHs from soils and snow during a short period of the austral summer.¹ Particularly, there is a lack of integrated assessments of PAH dynamics at the interface between land and ocean, not only at coastal Antarctica, but also for other regions. The study of the coupling among the atmosphere, land, and ocean requires an ambitious sampling strategy and the comprehensive assessment of the multiple interactions between the different compartments, including air–snow, air–soil, air–water, and land–ocean coupled fluxes. Furthermore, microbially driven processes such as the degradative and biological pumps may also play a role sequestering PAHs in the coastal waters and sediments as for other organic pollutants.^{16,17} The atmosphere–seawater cycling of PAHs is also of particular

Received: July 2, 2018

Revised: September 30, 2018

Accepted: October 2, 2018

Published: October 2, 2018

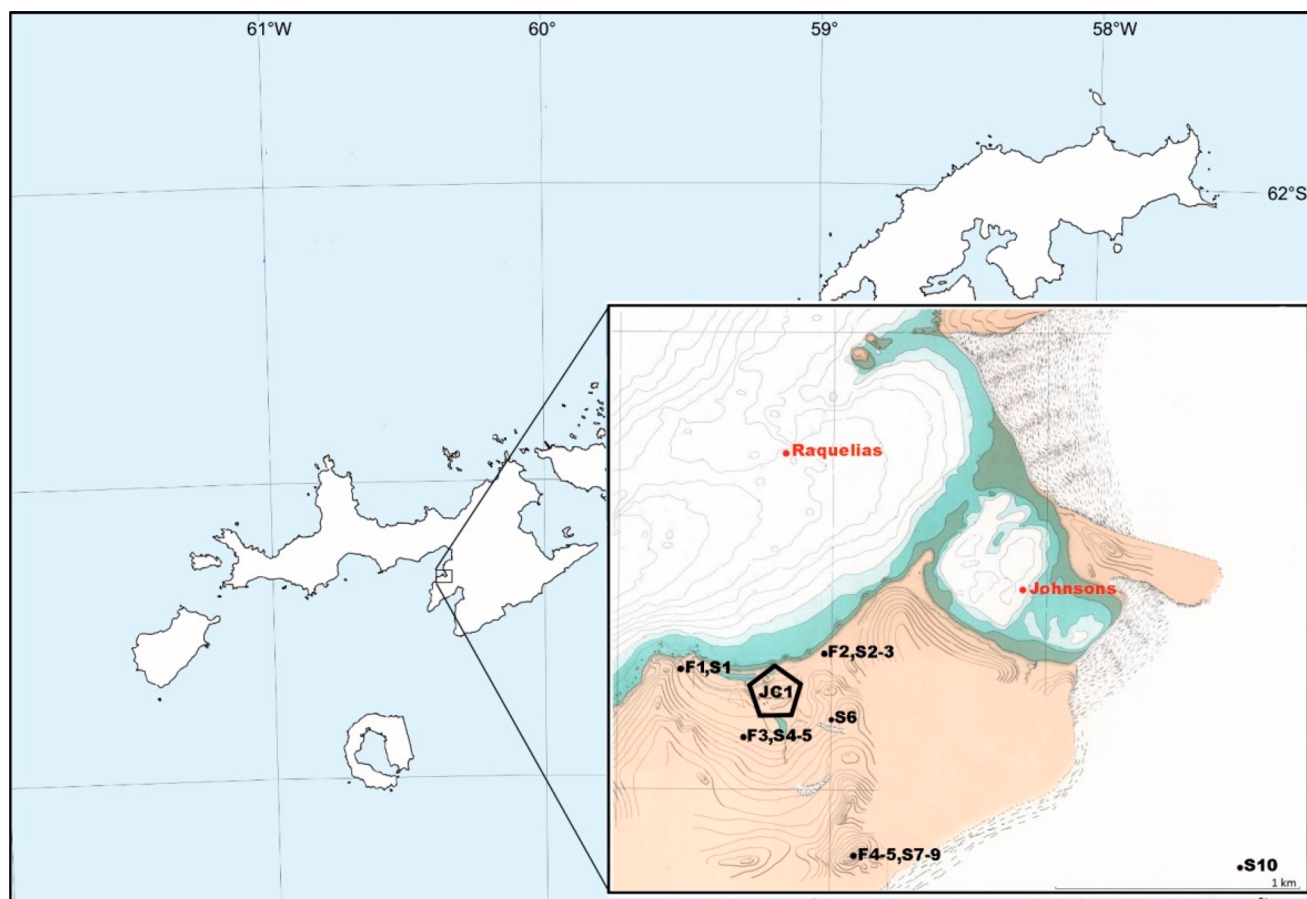


Figure 1. Sampling sites at Livingston Island. Five fugacity samplers were deployed to collect gas phase and gas phase equilibrated with snow/soil at F1–5 sites. Seawater and plankton samples were taken at Raquelias site ($62^{\circ} 39,438' S$, $60^{\circ} 23,306' W$) and Johnsons site ($62^{\circ} 39,556' S$, $60^{\circ} 22,132' W$). Snow samples were collected at S1–10 sites. JC1 means Juan Carlos I research station.

biogeochemical relevance due to the important role that the large pool of semivolatile aromatic-like compounds has in the marine carbon cycle.³ Although the behavior of PAHs in terms of atmospheric inputs and fate in the open ocean water column has been comprehensively studied recently,^{3,18} its dynamics in remote coastal regions remains uncharacterized. There are no previous concurrent assessments of air and seawater PAHs for the coastal Maritime Antarctica, and atmosphere–seawater fluxes have not been determined for this region.

The objectives of this work were to (i) provide, for the first time, concurrent multimedia concentrations in the Maritime Antarctica, including several relevant matrices (air, snow, seawater, plankton), (ii) assess the air–soil, air–snow, and air–water PAH dynamics at coastal Antarctica, and (iii) elucidate the main biogeochemical and climatic drivers of PAH fluxes and remobilization on land and in the water column.

MATERIALS AND METHODS

Site Description and Sampling. A three-month intensive sampling campaign (December 1, 2014 to March 1, 2015) was performed at Livingston Island ($62^{\circ} 39' S$, $60^{\circ} 23' W$), in the South Shetlands Archipelago, Antarctica. With two seasonal and small research stations located at South Bay of Livingston Island (Figure 1), this coastal area is under a lower anthropogenic pressure in comparison to other South Shetland Islands such as King's George.

Plankton and seawater sampling was conducted from a rigid inflatable boat at two sampling sites: Johnsons and Raquelias

(Figure 1). Johnsons site ($62^{\circ} 39,556' S$, $60^{\circ} 22,132' W$, 14 m depth) is located inside a shallow cove under the influence of several thawing rivers, 200 m away from the Johnsons glacier. Raquelias site ($62^{\circ} 39,438' S$, $60^{\circ} 23,306' W$, 40 m depth) is open to the South Bay of Livingston Island, at 1 km from the coast. Conductivity, temperature, density (CTD) depth profiles were taken immediately before sample collection and presented significant differences between sampling sites (Table S1, Supporting Information). Concurrent samples for seawater nutrient and bacterial biomass determination were also taken at the same sampling locations and dates, and stored at $-20^{\circ} C$ until their determination in the laboratory.

Twenty-six 100–120-L surface seawater samples (0.5–1 m depth) were collected in 20-L aluminum jerry cans and transported to the research station for their immediate filtration and extraction (Table S2, SI) as previously described.³ Briefly, seawater was filtered through precombusted GF/F glass fiber Whatmann filters ($0.7\text{-}\mu\text{m}$) before passing through precleaned XAD-2 (Supelco) packed stainless steel columns. This extraction was performed outside the laboratory in order to avoid potential contamination from indoor air, and for keeping the temperature at ambient levels (ranging from 0 to $4^{\circ} C$), thus not affecting the particle–water partitioning of PAHs. XAD-2 columns were stored at $4^{\circ} C$ for refrigerated transport until further analysis, while GF/F filters were wrapped in precombusted aluminum foil and stored at $-20^{\circ} C$ in airtight plastic bags until their analysis in the laboratory.

Twenty-six plankton samples were collected using a conical plankton net with a 50- μm mesh size by vertical hauls from bottom to surface (Table S3, SI). The sampling depths at Johnsons and Raquelias were 14 and 30 m (close to water column depth), respectively. The collected samples were filtered with precombusted and preweighted GF/D glass fiber Whatman filters (2.7- μm), and the filters were subsequently wrapped in precombusted aluminum foil and stored at $-20\text{ }^{\circ}\text{C}$ in airtight plastic bags until their analysis in the laboratory.

Ten surface (top 1–2 cm) snow samples were collected with a stainless steel shovel into Teflon bottles (Figure 1) and allowed to melt at $4\text{--}6\text{ }^{\circ}\text{C}$ for 24–48 h (Table S4, SI). Snow water samples followed the same procedure as surface seawater samples, also filtered outdoors to minimize temperature changes and/or contact with air from the research station.

Fifty-two ambient air and 51 surface fugacity samples were collected by means of a previously described fugacity sampler,^{19–21} deployed at 5 sampling sites (Figure 1, Tables S5–S7, SI). The fugacity sampler forces air to flow below a stainless-steel chamber separated 3 cm from the soil/snow surface allowing the air to equilibrate with the surface (soil or snow), thus providing a measure of the soil or snow fugacity. The fugacity sampler was initially developed for soils, and the air–soil equilibration is assessed by comparison of the concentrations using different flow rates.¹⁹ The comparison of the concentrations in air equilibrated with the snow surface at flow rates of 6 and 8 L min^{-1} with a second sampler operating at 10 L min^{-1} , showed comparable concentrations,¹ with a variability for 3–4 ring PAHs concentrations of 16% ($n = 4$, phenanthrene to pyrene). This variability is comparable to the variability of the concentrations obtained from side-by-side samplers over snow operating at the same flow rate (10 L min^{-1}). These results are consistent with PAHs in air and surface snow reaching equilibrium when the air is forced to flow below the fugacity sampler. The ambient air samples were collected simultaneously at 1.5-m height. Ambient air and surface fugacity samples were taken by passing the air through precombusted quartz fiber filters (GF/F) to remove dust particles, and through 10×2 cm precleaned polyurethane foam plugs (PUFs), where the compounds from the gas phase were retained. Sampling flow rates were slow (8–10 L min^{-1}) to allow air–surface equilibrium conditions below the sampler,¹⁹ with average sampled air volumes of 86 m^3 . The PUFs were subsequently stored at $-20\text{ }^{\circ}\text{C}$ in airtight precombusted glass vials.

Analytical Procedures. Plankton samples were Soxhlet-extracted with dichloromethane/hexane (1:1, v-v) during 24 h. Extracts were concentrated and fractionated with 25 mL of hexane and 40 mL of dichloromethane:hexane (1:3, v-v) on a 5 g of silica gel column (silica 60–200 mesh, activated at $250\text{ }^{\circ}\text{C}$ for 24 h) and 3 g of 3% deactivated neutral alumina column (aluminum oxide 90, activated at $250\text{ }^{\circ}\text{C}$ for 12 h). The dichloromethane/hexane fraction containing the PAHs was concentrated and solvent exchanged to iso-octane with a final volume of 100 μL .

XAD-2 columns enriched with the SVOCs from the snow and seawater dissolved phases were sequentially eluted with 200 mL of methanol, followed by 200 mL of dichloromethane and 100 mL of hexane using an axial piston pump with a 2 mL min^{-1} flow rate. The methanol fraction was concentrated and liquid–liquid-extracted with 50 mL of hexane for three times. The hexane extracts were dried over anhydrous sodium sulfate and combined with the dichloromethane and hexane fractions.

After reducing the volume, the extract followed the same fractionation process as the plankton samples. PUFs were Soxhlet-extracted with acetone/hexane (3:1, v-v) during 24 h. PUFs fractionation details can be found elsewhere.^{20,21}

PAH quantification was performed with an Agilent 6890 Series gas chromatograph coupled to a mass spectrometer Agilent 5973 (GCMS) operating in selected ion monitoring (SIM) and electron impact mode (EI). A 30-m capillary column (HP-5MS, 0.25 $\text{mm} \times 0.25\text{ }\mu\text{m}$ film thickness) was used. The oven temperature was increased to $90\text{ }^{\circ}\text{C}$ (held for 1 min), then increased to $175\text{ }^{\circ}\text{C}$ at $6\text{ }^{\circ}\text{C/min}$ (held for 4 min), increased to $235\text{ }^{\circ}\text{C}$ at $3\text{ }^{\circ}\text{C/min}$, increased to $300\text{ }^{\circ}\text{C}$ at $8\text{ }^{\circ}\text{C/min}$ (held for 8 min), and finally to $315\text{ }^{\circ}\text{C}$ for 5 min (held for 8 min). Injector and transfer line temperatures were 280 and $300\text{ }^{\circ}\text{C}$, respectively. Two μL of sample were injected in split less mode.

The following parent and alkylated PAHs were analyzed: acenaphthylene (Act), acenaphthene (Ace), fluorene (Flu), phenanthrene (Phe), anthracene (Ant), dibenzothiophene (DBT), fluoranthrene (Flt), pyrene (Pyr), benzo[a]anthracene (B[a]ant), chrysene (Cry), benzo[b]fluoranthene (B[b]f), benzo[k]fluoranthene (B[k]f), benzo[e]pyrene (B[e]pyr), benzo[a]pyrene (B[a]pyr), perylene (Pery), dibenzo[a,h]-anthracene (Dib[a,h]ant), benzo[g,h,i]perylene (B[g,h,i]per), indeno[1,2,3-cd]pyrene (In[1,2,3-cd]pyr), Benzo[ghi]-fluoranthrene (B[g,h,i]f), methylphenanthrenes (ΣMP , sum of 4 isomers), dimethylphenanthrenes (ΣDMP , sum of 7 isomers), methyl dibenzothiophenes (ΣMDBT , sum of 3 isomers), dimethyl dibenzothiophenes (ΣDMDBT , sum of 5 isomers), methylpyrenes (ΣMPyr , sum of 5 isomers), dimethylpyrenes (ΣDMPyr , sum of 8 isomers), and methylchrysenes (ΣMCry , sum of 2 isomers).

Nutrients (phosphate, nitrate plus nitrite, and ammonia) were analyzed by continuous flow analysis on a Bran+Luebbe (currently Seal Analytical) autoanalyzer following standard colometric methods.²²

Bacterial abundance was estimated from the gene copy numbers of the 16S gene by quantitative real-time polymerase chain reaction (qPCR) as described elsewhere.²³ Briefly, DNA was extracted from 47-mm diameter, 0.2- μm pore-size PTFE filters (Millipore) where we collected the biomass of 2 L of seawater prefiltered by GF/D (Whatmann) filters. Filters were soaked with lysis buffer (50 mM Tris HCl, 40 mM EDTA, 0.75 M Sucrose), incubated with lysozyme, proteinase K, and sodium dodecyl sulfate (SDS), and then nucleic acids were phenol-extracted as previously described.²⁴ Partial bacterial 16S gene fragments were quantified with SYBR Green (Thermo Scientific, Inc.) in one 96-well plate using primers 331F/518R in a Lightcycler 480 II (A.F. Hoffmann-La Roche AG, Inc.). The reaction mixture was thermocycled at $95\text{ }^{\circ}\text{C}$ for 7 min, 40 cycles at $95\text{ }^{\circ}\text{C}$ for 10 s, $60\text{ }^{\circ}\text{C}$ for 30 s, and $68\text{ }^{\circ}\text{C}$ for 90 s, followed by a final extension of 5 min at $68\text{ }^{\circ}\text{C}$. The plasmid vector pNORM was used as standard to normalize quantified genes. Each assay was run in triplicates including no template controls and standard curves spanning from 10^1 to 10^8 copies of standard 16S genes. Melting curves were obtained to confirm amplification specificity.

Quality Assurance/Quality Control. All containers, tubes, and connections used during sampling and chemical analysis were of stainless steel, glass, or PTFE, and they had been precleaned with acetone prior use in order to avoid contamination.

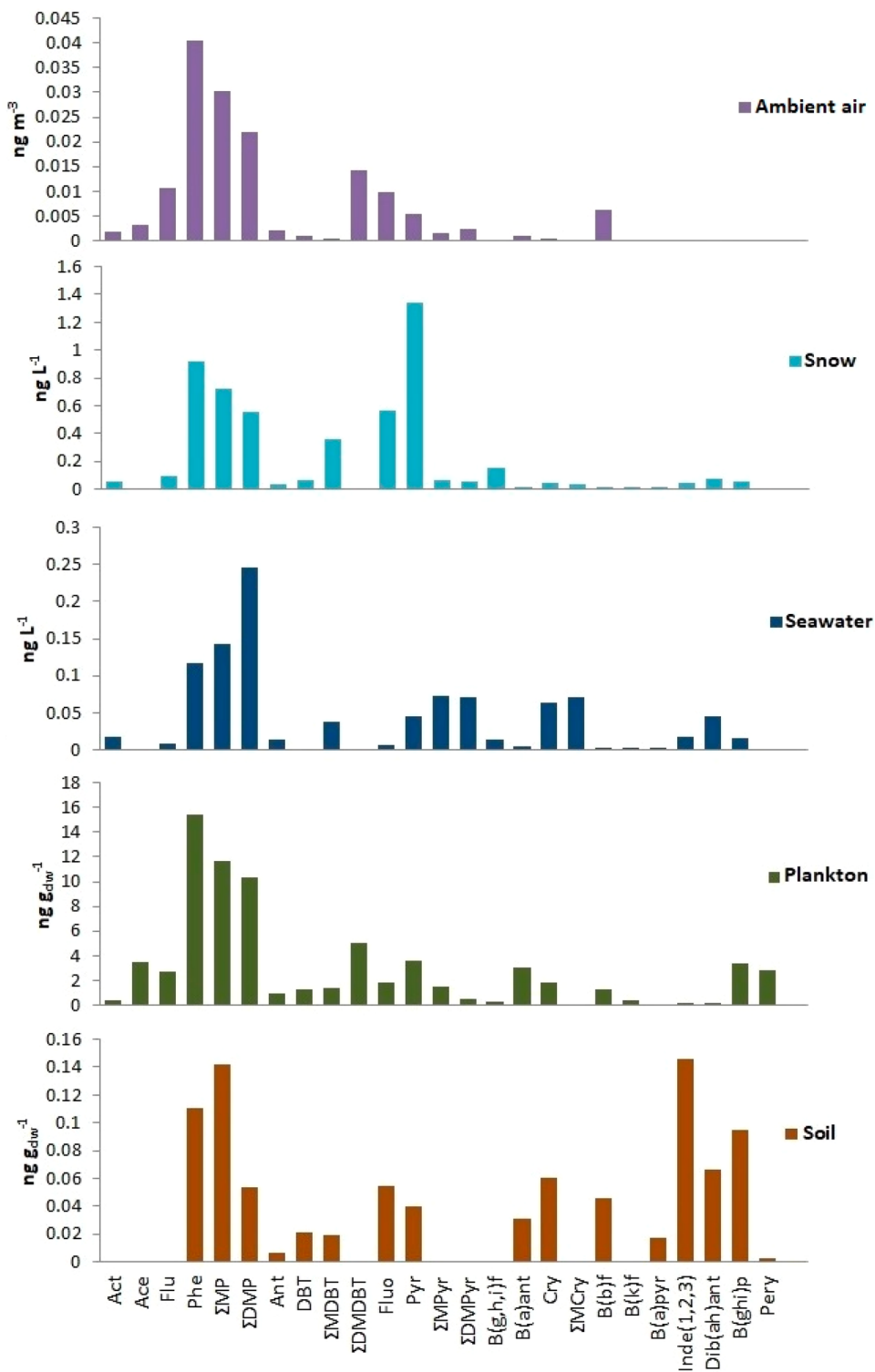


Figure 2. PAH average concentration profiles in air, snow, seawater, plankton, and soil matrices. Soil concentrations taken from Cabrerizo et al.⁸

To minimize contamination, all filters were precombusted at 450 °C over 4 h. XAD-2 was Soxhlet-extracted in methanol/dichlorometane (1:1) before column packing. The columns were pre-eluted with methanol, dichloromethane, and hexane, and the extracts were concentrated and injected to check for residual contamination. PUFs were precleaned with acetone/hexane (3:1, v:v) over 24 h and stored in airtight precombusted glass vials.

Field blanks consisted of GF/D filters, PUFs, and XAD-2 columns that followed the same process as the samples albeit without the pass of plankton, air, or water. Procedural and field blanks were analyzed with each batch of 4–6 samples to monitor potential contamination during sampling and extraction. The limits of quantification (LOQs) were defined as the mean concentration of field or procedural blanks, whichever higher, plus three times the standard deviation of the blank response. For the analytes which were not found in

procedural blanks, LOQs were derived from the lowest standard in the calibration curve.

Recoveries were monitored by a spike of perdeuterated PAHs standards (acenaphthene-*d*10, phenanthrene-*d*10, crysene-*d*12, and perylene-*d*12) prior to the extraction process and are provided in Table S8 (Supporting Information).

The measure of the copies of the 16S genes was done in triplicates. The standard deviation of the triplicate measurements was of 5%. For the nutrients analysis, detection limits (defined as three times the standard deviation of ten replicates at 50% diluted samples) were 0.003 μM for ammonia, 0.020 μM for phosphate, and 0.006 μM for nitrate. The coefficients of variations of all nutrients were <0.30%.

Statistical Analysis. All statistical analyses were performed with SPSS Statistics version 22.0 (IBM Corp.), and significance was set to $p < 0.05$. Correlations among concentrations and environmental variables were performed by Spearman rank-order analysis. Microbial controls on seawater and plankton concentrations were explored by multiple linear least-squares regressions.

RESULTS AND DISCUSSION

Soil–Air Exchange of PAHs. Average $\sum\text{PAHs}$ gas phase concentrations ($150 \pm 140 \text{ pg m}^{-3}$) were generally in a lower range (Table S5, SI) than in a previous atmospheric assessment in this region.¹ Similar gas phase $\sum\text{PAH}$ concentrations have been reported in the Arctic,^{25–28} even though with a large variability mainly due to differences in the number of targeted PAHs.

Although temperature constitutes one of the main drivers of gas-phase semivolatile organic compound concentrations,^{21,29} neither $\sum\text{PAHs}$, nor the individual PAH gas-phase concentrations were correlated with air temperature, as previously reported in semiurban/rural regions and over the ocean.^{30–32} The lack of temperature-dependent gas phase concentrations is consistent with air and surface (sea) at nonequilibrium and with an important contribution of atmospheric long-range transport in comparison to local sources.^{29,30} Potential PAH sources at coastal Antarctica are in situ emissions from local research stations and scientific/tourism cruises,⁸ revolatilization from soils and snow,¹ and biogenic sources related to organic matter degradation.^{1,33,34} The lower persistence of 2–4-ring PAHs than other SVOCs^{30,31} could also mask the influence of temperature on gas-phase concentrations.

PAH profiles in the gas phase were dominated by the lower molecular weight 3-ring PAHs, which accounted for $87 \pm 9.8\%$ of $\sum\text{PAHs}$, with Phe being the highest contributor ($30 \pm 8.2\%$) to $\sum\text{PAHs}$ (Figure 2), consistent with previous studies in polar regions.^{1,21}

The air fugacity (f_a , Pa) and the soil fugacity (f_s , Pa) of individual PAHs were calculated by

$$f_a = 10^{-9} C_A RT / MW \quad (1)$$

$$f_s = 10^{-9} C_{SA} RT / MW \quad (2)$$

where C_A is the measured ambient air concentration at 1.5 m height (ng m^{-3}), R is the gas constant ($8.314 \text{ Pa m}^3 \text{ mol}^{-1} \text{ K}^{-1}$), T is temperature (K), MW is the chemical molecular weight (g mol^{-1}), and C_{SA} (ng m^{-3}) is the gas-phase concentration that had been equilibrated with the soil/snow surface (Tables S6, SI), as measured using the soil fugacity

sampler. With this approach, C_{SA} is directly proportional to the surface fugacity.

C_{SA} PAH profiles had a higher proportion of low MW PAHs than C_A . 3-Ring PAHs contributed $95 \pm 2.1\%$ to $\sum\text{PAHs}$, and the average Phe contribution to $\sum\text{PAHs}$ was $40 \pm 11\%$. This is consistent with the low concentrations of aerosol black carbon and associated PAHs in the region,¹ as black carbon is especially enriched in high MW PAHs. Furthermore, previous studies reported soils as a source of volatile PAHs in polar regions.^{1,21,34} C_{SA} was not correlated with the inverse of temperature, as for ambient air. This contrasts with the influence of temperature observed for the soil fugacity of some PAHs in an arctic urban and coastal site.²¹ This lack of correlation is likely due to the narrow range of the mean ambient temperatures at this region of the Maritime Antarctica during summer (averages ranging from 0.26 to 2.6 °C) (Table S7, SI).

The least-squares linear regression of $\text{Log } f_s$ versus $\text{Log } f_a$ showed that the PAHs fugacity in air and soils were closely correlated (Figure 3). This correlation confirms a close coupling of air and soil PAH fugacities, and is consistent with previous reports in temperate and European polar regions.^{1,21,34,35}

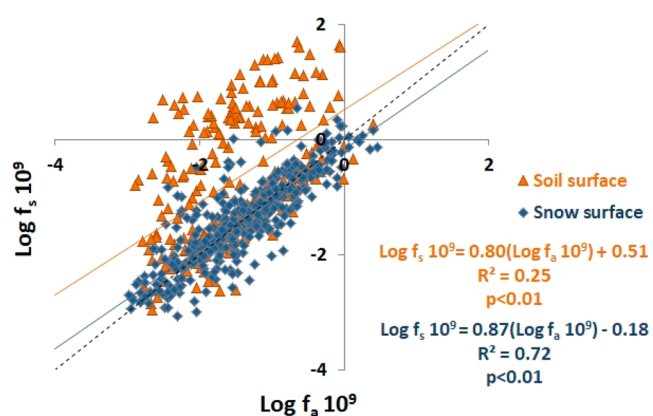


Figure 3. PAHs fugacity in air (f_a , Pa) versus fugacity in soil or snow (f_s , Pa).

Fugacity (f_s/f_a) ratios were evaluated to determine the direction of soil–air exchanges of PAHs (Figure 4, Table S9, SI), where values higher and lower than 1 indicate net volatilization and deposition of the chemical, respectively. Seventy-two percent of f_s values were higher than the simultaneously measured f_a , which indicates a dominance of PAH volatilization processes on the air–soil exchange. Because of uncertainty in the measurements, equilibrium is considered for $\text{Ln } f_s/f_a$ values between -1.2 and 0.53 .²⁰ Bare soil and soil with vegetation presented notable differences in f_s/f_a ratios (Figure 4), with bare soil–air coupling being close to equilibrium during the sampling campaign. Conversely, net volatilization from soil with vegetation was observed for most of the target compounds (Figure 4). These differences are likely related with higher soil organic matter (SOM) content in soil with vegetation cover. Furthermore, the statistically significant least-squares linear regressions of $\text{Ln } f_s/f_a$ versus $\text{Log } K_{OA}$ showed higher volatilization for the less hydrophobic compounds (Figure 4). The fact that soils covered with vegetation showed higher volatilization fluxes than bare soils could be due to a number of factors. There is a potential

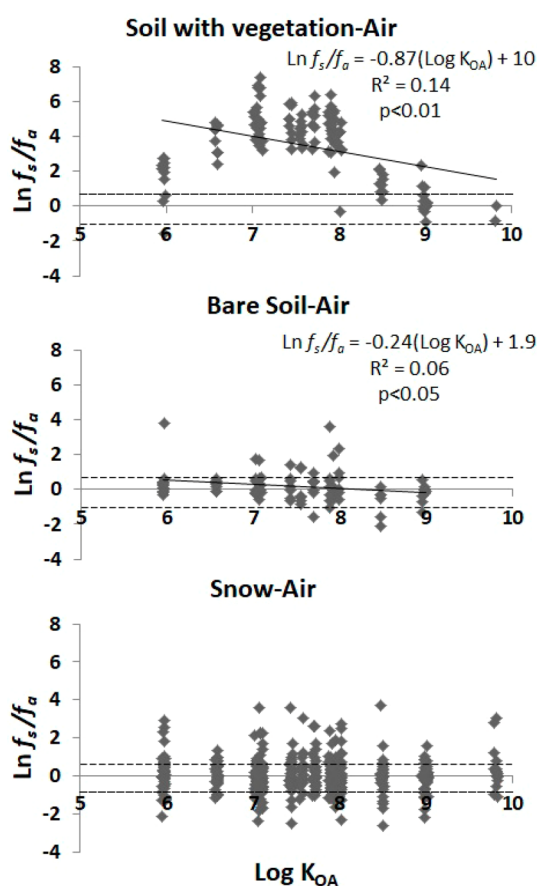


Figure 4. Variation of the soil/snow–air fugacity ratios ($\text{Ln } f_s/f_a$) versus the octanol–air partition coefficient (K_{OA}). The horizontal dashed lines mark ratios -1.2 and 0.53 , the interval for air–surface equilibrium.

biogenic production of the more volatile PAHs contributing to PAHs volatilization by degradation of diterpenes and enhanced SOM digestion by fungal acids, which have been suggested as mechanisms that would mediate in this process.^{1,20,33} Indeed, terpenes from plant detritus can aromatize during aging, converting to low MW PAHs.^{36,37} The fugacity amplification of PAHs in snowmelt is retained in the soil organic carbon; as soils covered with vegetation have higher SOM, this is translated to higher soil concentrations of PAHs. The high soils concentrations can be translated to a high soil fugacity in the case that there is a decrease of the fugacity capacity of soils. This fugacity capacity is related to the soil organic carbon content. Soil respiration converts soil organic carbon to CO_2 . Soil respiration is an example of a solvent depletion amplifying the fugacity, as has been described by other processes such as snow melting.³⁸ In the South Shetland region, it has been shown that soil respiration in soils covered by lichens is significantly higher than that in bare soils, and that soil respiration is significantly increased after snow melting.³⁹ This solvent depletion mechanism is consistent with the higher PAH fugacity in soils covered with lichens than in soils without vegetation (lower SOM and solvent depletion by respiration).

Snow–Air Partitioning of PAHs. \sum PAHs average concentrations in snow ranged from 0.39 to 9.2 ng L^{-1} (Table S4, SI), and were not significantly correlated to the snow density or age. Similar \sum PAHs concentrations have been

previously reported in coastal surface snow from the Northern Victoria Land,¹⁴ and in snow/ice cores at Talos Dome.¹⁰

PAH concentrations 1–2 orders of magnitude higher were observed on King George Island,¹³ which is likely due to a higher presence of local sources in the Fildes Peninsula, such as 9 permanent research stations, a small airport, and a high incidence of cruise tourism, which is residual at Livingston Island. Similarly, high levels of PAHs have been reported in snow from Victoria Land (140 ng L^{-1}), particularly high for naphthalene (125 ng L^{-1}), which was attributed to local contamination from a Twin Otter (aircraft) refuelling point.¹⁴ These examples of the presence of local contamination in soils or snow were suggested as evidence that LRAT did not contribute significantly to recent snow contamination in other regions.⁴⁰ However, at Livingston island, there was no significant correlation between PAH snow concentrations and the distance to JCI Station. On the other hand, PAH snow concentrations reported in the Arctic and remote regions from the northern hemisphere are generally 1 or 2 orders of magnitude higher than in Antarctica, which has been suggested as a result of limited inputs of air masses from lower latitudes due to the atmospheric dynamics of the Antarctic region.⁴¹ However, PAH atmospheric concentrations reported here and by Cabrerizo et al.¹ are comparable to those reported for the Arctic,^{25–28} which is due to preferential air mass transport from South America and northern latitudes affecting primarily the northern Antarctic Peninsula and South Shetland islands during the austral summer.⁴² As we have shown in a related paper reporting the dynamics for perfluoroalkyl substances during the same sampling campaign,⁴³ the back trajectories for snow deposition events are from air masses from northern latitudes and South America. The rest of the Antarctic continent has a strong influence of katabatic winds.

Snow–air partitioning constants (K_{SA}) were calculated as

$$K_{SA} = \frac{C_S}{C_{SA}} \quad (3)$$

where C_S (ng m^{-3}) is the individual PAH concentration in surface snow and C_{SA} (ng m^{-3}) is the gas-phase concentration that has been equilibrated with the snow surface as measured using the soil–snow fugacity sampler (Table S6, SI). PAHs $\text{Log } K_{SA}$ presented a statistically significant correlation with its Log vapor pressure ($r_s^2 = -0.21$, $p < 0.001$), consistent with a lower MW PAHs profile in the gas phase equilibrated with the snow surface than in its correspondent snow sample (Figure 2). Furthermore, as with soil fugacity, snow fugacity was closely correlated to air fugacity and the significant least-squares regression between them explained 72% of the variability (Figure 3).

However, f_s/f_a ratios presented no correlation with K_{OA} nor with vapor pressure, and no clear tendency toward volatilization or net deposition could be established for PAHs regardless of hydrophobicity (Figure 4), showing close to snow–air equilibrium. This result contrasts with the PAHs net volatilization from snow observed for a short period in 2009 at the same region.¹ Even though the temperature ranges in the 2008–09 and 2014–15 sampling campaigns were overlapping (0.5 to $3.5 \text{ }^\circ\text{C}$), during the 2014–15 campaign there was a much larger snow cover of the coastal zone, and a larger number of snow deposition events. Snowflakes may equilibrate with the gas phase in terms of PAHs fugacity during their fall³⁸ and, thus, the several snow deposition events during

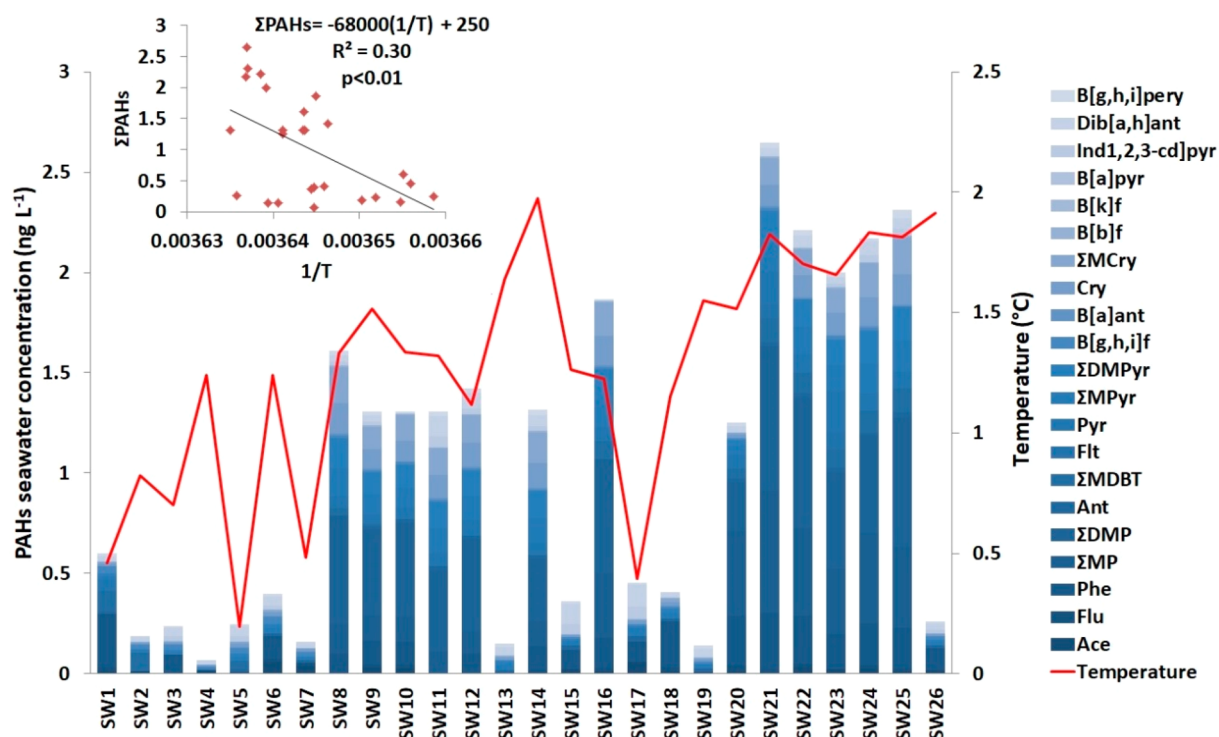


Figure 5. PAH seawater concentrations (ng L^{-1}) at coastal Livingston Island, and ambient temperature during the austral summer. The sampling for seawater started in December (sample SW1) and lasted until February (sample SW26).

the 2014–15 campaign may have contributed to keeping the surface snow fugacity close to equilibrium with the atmosphere. Conversely, in the absence of snow events, and due to melting/freezing occurring daily, it is likely that surface snow loses part of its fugacity capacity, inducing a larger surface snow fugacity than in ambient air, as observed in the 2008–09 campaign. These differences between the two campaigns, reflected in the behavior and fluxes of PAHs, are likely due to the different amount of snowfall and the timing of snowmelt between the two campaigns.

PAHs in the Coastal Water Column. Average Σ PAHs seawater and plankton concentrations were $1.0 \pm 0.82 \text{ ng L}^{-1}$ and $80 \pm 46 \text{ ng g}_{\text{dw}}^{-1}$, respectively (Tables S2–S3, SI), with no significant differences between the two sampling sites. PAH seawater and plankton profiles were dominated by the lower molecular weight compounds; 3-ring PAHs represented on average $50 \pm 17\%$ and $73 \pm 9.0\%$ of the profile, respectively, with Phe being the average highest contributor to Σ PAHs in both matrices (Figure 2). The high predominance of low MW PAHs is consistent with their higher aqueous solubility, and the low concentrations of aerosol black carbon and of high MW PAHs in the atmosphere.¹ The profile in the dissolved and plankton phase reflects the gas phase.

These PAH seawater concentrations and profiles are comparable to those in previous reports on Prydz Bay² and Terra Nova Bay.¹² Similar low PAH seawater concentrations can be found in the open ocean.³ To our knowledge, there are no previous reports of PAHs in plankton for the Maritime Antarctica. PAHs concentrations reported in suspended particle matter and biota from Potter Cove (King George Island) are not significantly different.¹¹

PAH concentrations in plankton were not significantly correlated with those in seawater. This is likely due to the fact that while seawater was sampled from the surface, plankton

samples integrated the water column from 14 and 30 m depth for the Johnsons and Raquelias sampling sites, respectively. A concurrent sampling on perfluoroalkylated substances concentrations in seawater and plankton also did not show a significant correlation.⁴³

Σ PAHs concentrations in seawater increased over the sampling campaign period, from late spring to late summer, and were significantly correlated with seawater temperature (Figure 5). This increase in Σ PAHs concentrations is consistent with an increase of fresh water discharge from ice and snowmelt during the austral summer, as ambient temperature fluctuated from below freezing temperatures to few positive Celsius degrees (Figure 5). Snow Σ PAHs concentrations were significantly higher than those of seawater, and fugacity ratios showed no net volatilization from snow, as there was close to equilibrium condition for air–snow exchange (Figure 4), suggesting that most PAHs in snow are transferred to coastal water through snowmelt. Furthermore, 4–5 ringed Σ PAHs concentrations in seawater were also correlated with seawater temperature (Figure S1, SI). This is consistent with the role of fresh water (snowmelt) discharge removing previously deposited aerosol-phase PAHs scavenged by wet (snow and rain) deposition. However, Σ PAHs concentrations in coastal seawater were not significantly correlated with salinity, which is likely due to its narrow range (33–34 PSU, Table S1, SI), the tidal dynamics renewing and mixing the top seawater in South Bay, or that the increase of concentration of PAHs in surface waters due to snowmelt inputs is lost due to volatilization, the biological pump, or degradation.

Diffusive air–water fluxes are the main driver for light (2–4 rings) PAHs in the gas and dissolved phase exchange.^{3,31} Diffusive air–water fluxes (F_{AW}) were calculated following the two-film resistance model:⁴⁴

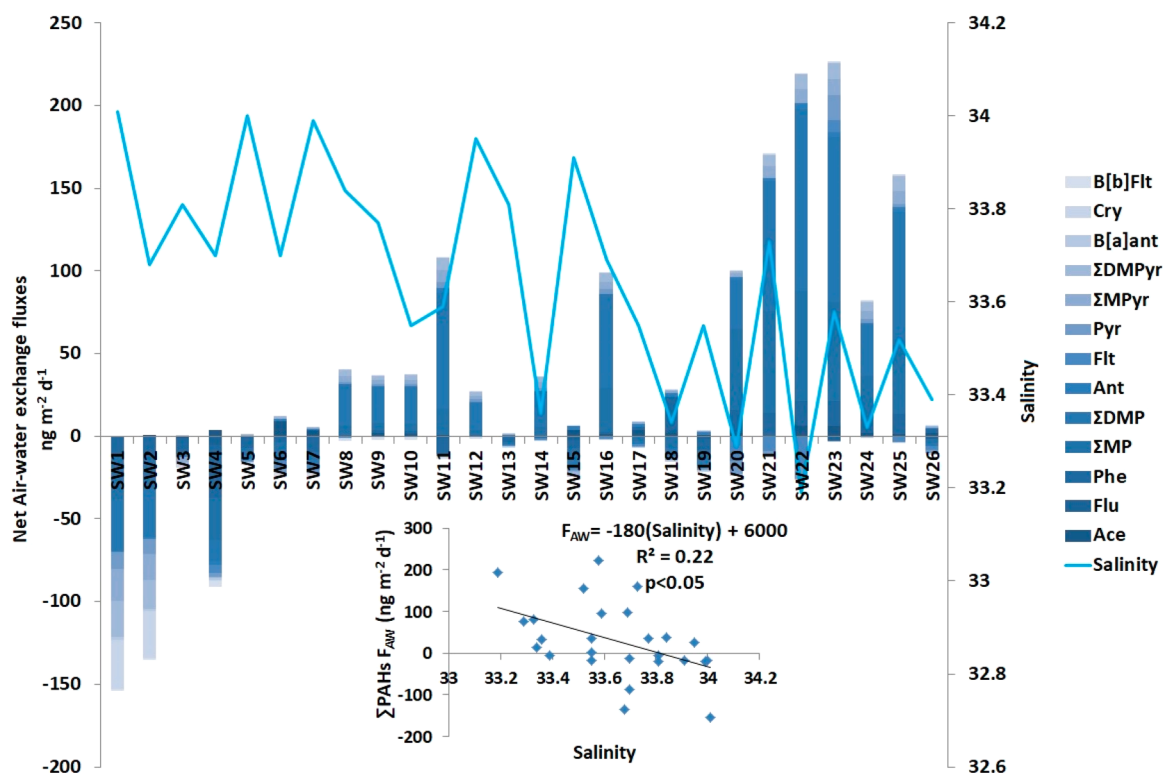


Figure 6. PAH net air–water exchange fluxes (F_{AW} , $\text{ng m}^{-2} \text{d}^{-1}$) and salinity during the three-month sampling campaign. Inner panel shows the correlations of F_{AW} with surface seawater salinity.

$$F_{AW} = F_{AWabs} - F_{AWvol} = k_{AW} \left(\frac{C_A}{H'} - C_W \right) \quad (4)$$

where C_W is the dissolved phase PAH concentration (ng m^{-3}), H' is the temperature and salinity corrected dimensionless Henry's law constant,⁴⁵ and k_{AW} is the air–water mass transfer rate (m d^{-1}).⁴⁶

Gross absorption fluxes (F_{AWabs}) ranged from 6.0 to 170 $\text{ng m}^{-2} \text{d}^{-1}$ (Table S10, SI), and, although H' is temperature dependent, they did not present a significant correlation with seawater or air temperature. On the other hand, as seawater PAH concentrations did present a significant correlation with seawater temperatures (Figure 5), so did the gross volatilization fluxes, F_{AWvol} , which ranged from 0.79 to 260 $\text{ng m}^{-2} \text{d}^{-1}$ (Table S11, SI). Furthermore, gross volatilization fluxes showed significant inverse correlations with salinity (Table S14, SI), consistent with snowmelt driving an increase of the losses due to volatilization.

The resulting net air–water fluxes (F_{AW} , Table S12, SI) followed a remarkable shift during the sampling campaign, from the net deposition of 150 $\text{ng m}^{-2} \text{d}^{-1}$ during the late spring, to the net volatilization of 220 $\text{ng m}^{-2} \text{d}^{-1}$ during the late summer. The net air–water fluxes showed significant correlations with seawater salinity and temperature (Table S13–14, SI). This net volatilization contrasts with the dominance of absorption fluxes observed in open sea regions such as the tropical and subtropical Atlantic, Pacific, and Indian oceans,³ as well as the Mediterranean and Black Seas.¹⁸

The least-squares linear regression of F_{AW} versus salinity (Figure 6), indicates that volatilization is enhanced by the freshwater discharge due to snow/ice melting, which is consistent with the high PAH concentrations in snow contributing to increase the concentrations in seawater during

the snowmelt season. As there is no net volatilization from snow (Figure 3), PAHs are transferred to soil organic matter or coastal seawater. Similar latitudinal and seasonal shifts in the air–seawater–water exchange have been previously reported and linked to the contributions from ice/snowmelt for other SVOCs in Antarctica.^{47–49} Indeed, glacier snowmelt has also been recently highlighted as a secondary source of SVOCs to the Antarctic marine ecosystem.^{50,51}

Therefore, the overall dynamics of PAHs in coastal Antarctica is consistent with an important role of snow deposition of PAHs, which are accumulated in the snowpack during winter. Surface snow is close to equilibrium with the gas-phase concentrations. The concentrations of aerosols are extremely low in this region, especially for black carbon aerosols,⁵² and dry deposition does not drive high concentrations of high MW PAHs to coastal soils, snow, and seawater. Nevertheless, their low concentrations in seawater are correlated with salinity (Figure S1, SI). During the austral summer melting, the PAHs in snowmelt will be either accumulated in the soil organic matter (especially in soils covered by vegetation), and if not retained in soils, PAHs will be transferred to coastal seawater. Glacier melting will also introduce historic PAHs burden to seawater and contribute to salinity decrease. Either in soil organic matter, or in coastal seawater, the fugacity amplification of the original snow results in a fugacity amplification in soil organic matter or surface seawater, and thus it results in a volatilization of PAHs back to the atmosphere.

The main Antarctic sinks will be the transfer of PAHs to coastal sediments due to the biological pump, as well as microbial degradation in seawater and soils,⁵³ and potential increasing concentrations in the different Antarctic matrixes. Nitrate showed a decrease of concentrations during the austral

summer, with direct correlations with salinity and temperature (Figure S2, SI), consistent with an increase of primary productivity that fueled bacterial activities.⁵⁴ Phosphate concentrations also increased during high turbidity periods, maybe related to inputs of glacier-derived material (Figure S3, SI). Bacterial abundances were concurrently measured with the PAHs and nutrient concentrations in seawater, and the rates of increase/decrease of bacterial cells estimated from consecutive measurements of bacterial biomass. Bacterial abundance was correlated with ammonium concentrations ($r^2 = 0.47$, $p < 0.01$), that increased from the low values during the first sampling periods, to higher levels for most of the rest of the austral summer (Table S1, SI). Ammonium may have originated from organic matter inputs from land, which is consistent with its covariability with bacteria, and the direct correlation between \sum PAHs in the dissolved phase and ammonium concentrations (Figure S4, SI). Previous reports have shown that the concentrations of 2–3 ring PAHs in plankton (as surrogates of the levels in the water column) decrease with the planktonic biomass,⁵⁵ which has been suggested as evidence of microbial degradation. PAH concentrations of lower MW PAHs in coastal Antarctic plankton also decreased with biomass as in previous reports⁵⁵ (Figure S5, SI). In addition, the concentrations of 2–3 ring PAHs in plankton were correlated by means of a multiple linear least-squares regression with the bacterial abundance for the previous time period, temperature, and the interaction of both ($r^2 = 0.57$, $p < 0.5$). These results provide evidence that microbial degradation and temperature play key roles by controlling the water column concentrations through snow-melting enhanced inputs to the coastal zone (temperature driven) and consumption of lighter PAHs in the water column. Polar marine bacteria have been described to have the potential for degrading PAHs using these chemicals as a source of carbon.^{56,57} It is unclear to which degree the Antarctica is a net sink of PAHs, as the integrated fluxes to the sediment, and of degradation in the water column could not be constrained. Microbial degradation of PAHs in coastal soils is feasible, but experiments have shown that this is an extremely slow process at low temperatures.⁵⁸ Therefore, the marine biological and degradative pumps will account for the major Antarctic sinks, as the temperature-driven net volatilization of PAHs described here will recycle an important fraction of PAHs back to the atmosphere, and thus susceptible of further transport and deposition. In this case, Antarctica would just be one stop in the grass-hopping journey.

■ ASSOCIATED CONTENT

📄 Supporting Information

The Supporting Information is available free of charge on the ACS Publications website at DOI: 10.1021/acs.est.8b03640.

Tables S1–S14 and Figures S1–S5 (PDF)

■ AUTHOR INFORMATION

Corresponding Author

*E-mail: jordi.dachs@idaea.csic.es; phone: +34 93 4006170; fax: +34 93 2045904.

ORCID

Maria Vila-Costa: 0000-0003-1730-8418

Jordi Dachs: 0000-0002-4237-169X

Notes

The authors declare no competing financial interest.

■ ACKNOWLEDGMENTS

Inorganic nutrient analyses were performed by Mrs. M. I. Abad in coordination with Dr. E. Berdalet (Head of the Service) at the “Nutrient Analysis Service” of the ICM (CSIC). We thank F. Cerqueria and A. Martinez for support with DNA analysis. This work was supported by Spanish Ministry of Science to P.C. through a predoctoral fellowship, by Fundación BBVA award to M.V.C., European Commission to A.C. through a Marie Curie international outgoing fellowship, and by the Spanish MINECO through projects REMARCA (CTM2012-34673) and ISOMICS (CTM2015-65691-R). The research group of Global Change and Genomic Biogeochemistry is supported by the Catalan Government (2017SGR800).

■ REFERENCES

- (1) Cabrerizo, A.; Galbán-Malagón, C.; Del Vento, S.; Dachs, J. Sources and fate of polycyclic aromatic hydrocarbons in the Antarctic and Southern Ocean atmosphere. *Glob. Biogeochem. Cycles* **2014**, *28*, 1424–1436.
- (2) Cai, M.; Liu, M.; Hong, Q.; Lin, J.; Huang, P.; Hong, J.; Wang, J.; Zhao, W.; Chen, M.; Cai, M.; Ye, J. Fate of Polycyclic Aromatic Hydrocarbons in Seawater from the Western Pacific to the Southern Ocean (17.5°N to 69.2°S) and Their Inventories on the Antarctic Shelf. *Environ. Sci. Technol.* **2016**, *50* (17), 9161–9168.
- (3) Gonzalez-Gaya, B.; Fernandez-Pinos, M.-C.; Morales, L.; Mejanelle, L.; Abad, E.; Pina, B.; Duarte, C. M.; Jimenez, B.; Dachs, J. High atmosphere-ocean exchange of semivolatile aromatic hydrocarbons. *Nat. Geosci.* **2016**, *9* (6), 438–442.
- (4) Bostrom, C. E.; Gerde, P.; Hanberg, A.; Jernström, B.; Johansson, C.; Kyrklund, T.; Rannug, A.; Törnqvist, M.; Victorin, K.; Westerholm, R. Cancer risk assessment, indicators, and guidelines for polycyclic aromatic hydrocarbons in the ambient air. *Environ. Health Perspect.* **2002**, *110*, 451–488.
- (5) Hylland, K. Polycyclic aromatic hydrocarbon (PAH) ecotoxicology in marine ecosystems. *J. Toxicol. Environ. Health, Part A* **2006**, *69*, 109–123.
- (6) Lei, Y. D.; Wania, F. Is rain or snow a more efficient scavenger of organic chemicals? *Atmos. Environ.* **2004**, *38* (22), 3557–3571.
- (7) Tin, T.; Fleming, Z. L.; Hughes, K. A.; Ainley, D. G.; Convey, P.; Moreno, C. A.; Pfeiffer, S.; Scott, J.; Snape, I. Impacts of local human activities on the Antarctic environment. *Antarct. Sci.* **2009**, *21* (01), 3–33.
- (8) Cabrerizo, A.; Dachs, J.; Barceló, D.; Jones, K. C. Influence of organic matter content and human activities on the occurrence of organic pollutants in Antarctic soils, lichens, grass, and mosses. *Environ. Sci. Technol.* **2012**, *46* (3), 1396–1405.
- (9) Fuoco, R.; Giannarelli, S.; Wei, Y.; Abete, C.; Francesconi, S.; Termine, M. Polychlorobiphenyls and polycyclic aromatic hydrocarbons in the sea-surface micro-layer and the water column at Gerlache Inlet (Antarctica). *J. Environ. Monit.* **2005**, *7*, 1313–1319.
- (10) Fuoco, R.; Giannarelli, S.; Onor, M.; Ghimenti, S.; Abete, C.; Termine, M.; Francesconi, S. A snow/firn four-century record of polycyclic aromatic hydrocarbons (PAHs) and polychlorobiphenyls (PCBs) at Talos Dome (Antarctica). *Microchem. J.* **2012**, *105*, 133–141.
- (11) Curtosi, A.; Pelletier, E.; Vodopivec, C. L.; Mac Cormack, W. P. Distribution of PAHs in the water column, sediments and biota of Potter Cove, South Shetland Islands, Antarctica. *Antarct. Sci.* **2009**, *21* (4), 329–339.
- (12) Stortini, A. M.; Martellini, T.; Del Bubba, M.; Lepri, L.; Capodaglio, G.; Cincinelli, A. n-Alkanes, PAHs and surfactants in the sea surface microlayer and sea water samples of the Gerlache Inlet sea (Antarctica). *Microchem. J.* **2009**, *92* (1), 37–43.
- (13) Na, G.; Liu, C.; Wang, Z.; Ge, L.; Ma, X.; Yao, Z. Distribution and characteristic of PAHs in snow of Fildes Peninsula. *J. Environ. Sci.* **2011**, *23*, 1445–1451.

- (14) Vecchiato, M.; Argiriadis, E.; Zambon, S.; Barbante, C.; Toscano, G.; Gambaro, A.; Piazza, R. Persistent Organic Pollutants (POPs) in Antarctica: occurrence in continental and coastal surface snow. *Microchem. J.* **2015**, *119*, 75–82.
- (15) Bengtson Nash, S. Persistent organic pollutants in Antarctica: current and future research priorities. *J. Environ. Monit.* **2011**, *13*, 497–504.
- (16) Galbán-Malagón, C. J.; Del Vento, S.; Cabrerizo, A.; Dachs, J. Factors affecting the atmospheric occurrence and deposition of polychlorinated biphenyls in the Southern Ocean. *Atmos. Chem. Phys.* **2013**, *13* (23), 12029–12041.
- (17) Galbán-Malagón, C.; Cabrerizo, A.; Caballero, G.; Dachs, J. Atmospheric occurrence and deposition of hexachlorobenzene and hexachlorocyclohexanes in the Southern Ocean and Antarctic Peninsula. *Atmos. Environ.* **2013**, *80*, 41–49.
- (18) Castro-Jiménez, J.; Berrojalbiz, N.; Wollgast, J.; Dachs, J. Polycyclic aromatic hydrocarbons (PAHs) in the Mediterranean Sea: atmospheric occurrence, deposition and decoupling with settling fluxes in the water column. *Environ. Pollut.* **2012**, *166*, 40–47.
- (19) Cabrerizo, A.; Dachs, J.; Barcelo, D. Development of a Soil Fugacity Sampler for Determination of Air–Soil Partitioning of Persistent Organic Pollutants under Field Controlled Conditions. *Environ. Sci. Technol.* **2009**, *43* (21), 8257–8263.
- (20) Cabrerizo, A.; Dachs, J.; Moeckel, C.; Ojeda, M. J.; Caballero, G.; Barceló, D.; Jones, K. C. Ubiquitous net volatilization of polycyclic aromatic hydrocarbons from soils and parameters influencing their soil-air partitioning. *Environ. Sci. Technol.* **2011**, *45* (11), 4740–4747.
- (21) Casal, P.; Castro-Jiménez, J.; Pizarro, M.; Katsoyiannis, A.; Dachs, J. Seasonal soil/snow-air exchange of semivolatile organic pollutants at a coastal arctic site (Tromsø, 69° N). *Sci. Total Environ.* **2018**, *636*, 1109–1116.
- (22) Armstrong, F. A. J.; Stearns, C. R.; Strickland, J. D. H. The measurement of upwelling and subsequent biological processes by means of the Technicon AutoAnalyzer and associated equipment. *Deep-Sea Res. Oceanogr. Abstr.* **1967**, *14*, 381–389.
- (23) Tamminen, M.; Karkman, A.; Lõhmus, A.; Muziasari, W. I.; Takasu, H.; Wada, S.; Suzuki, S.; Virta, M. Tetracycline resistance genes persist at aquaculture farms in the absence of selection pressure. *Environ. Sci. Technol.* **2011**, *45* (2), 386–391.
- (24) Vila-Costa, M.; Barberan, A.; Auguet, J. C.; Sharma, S.; Moran, M. A.; Casamayor, E. O. Bacterial and archaeal community structure in the surface microlayer of high mountain lakes examined under two atmospheric aerosol loading scenarios. *FEMS Microbiol. Ecol.* **2013**, *84* (2), 387–397.
- (25) Halsall, C. J.; Barrie, L. A.; Fellin, P.; Muir, D. C. G.; Billeck, B. N.; Lockhart, L.; Rovinsky, F. Y.; Kononov, E. Y.; Pastukhov, B. Spatial and temporal variation of polycyclic aromatic hydrocarbons in the Arctic atmosphere. *Environ. Sci. Technol.* **1997**, *31* (12), 3593–3599.
- (26) Hung, H.; Blanchard, P.; Halsall, C. J.; Bidleman, T. F.; Stern, G. A.; Fellin, P.; Muir, D. G. C.; Barrie, L. A.; Jantunen, L. M.; Helm, P. A. Temporal and spatial variabilities of atmospheric polychlorinated biphenyls (PCBs), organochlorine (OC) pesticides and polycyclic aromatic hydrocarbons (PAHs) in the Canadian Arctic: Results from a decade of monitoring. *Sci. Total Environ.* **2005**, *342* (1–3), 119–144.
- (27) Wang, R.; Tao, S.; Wang, B.; Yang, Y.; Lang, C.; Zhang, Y. X.; Hu, J.; Ma, J. M.; Hung, H. Sources and pathways of polycyclic aromatic hydrocarbons transported to alert, the Canadian High Arctic. *Environ. Sci. Technol.* **2010**, *44* (3), 1017–1022.
- (28) Ma, Y.; Xie, Z.; Yang, H.; Möller, A.; Halsall, C.; Cai, M.; Sturm, R.; Ebinghaus, R. Deposition of polycyclic aromatic hydrocarbons in the North Pacific and the Arctic. *J. Geophys. Res.* **2013**, *118* (11), 5822–5829.
- (29) Wania, F.; Haugen, J.-E.; Lei, Y. D.; Mackay, D. Temperature Dependence of Atmospheric Concentrations of Semivolatile Organic Compounds. *Environ. Sci. Technol.* **1998**, *32* (8), 1013–1021.
- (30) Gigliotti, C. L.; Dachs, J.; Nelson, E. D.; Brunciak, P. A.; Eisenreich, S. J. Polycyclic aromatic hydrocarbons in the New Jersey coastal atmosphere. *Environ. Sci. Technol.* **2000**, *34* (17), 3547–3554.
- (31) Gigliotti, C. L.; Brunciak, P. A.; Dachs, J.; Glenn, T. R.; Nelson, E. D.; Totten, L. A.; Eisenreich, S. J. Air–water exchange of polycyclic aromatic hydrocarbons in the New York–New Jersey, USA, Harbor Estuary. *Environ. Toxicol. Chem.* **2002**, *21* (2), 235–244.
- (32) Nizzetto, L.; Lohmann, R.; Gioia, R.; Jahnke, A.; Temme, C.; Dachs, J.; Herckes, P.; Guardo, A. D.; Jones, K. C. PAHs in air and seawater along a north-south Atlantic transect: trends, processes and possible sources. *Environ. Sci. Technol.* **2008**, *42* (5), 1580–1585.
- (33) Wilcke, W. Global patterns of polycyclic aromatic hydrocarbons (PAHs) in soil. *Geoderma* **2007**, *141* (34), 157–166.
- (34) Cabrerizo, A.; Tejado, P.; Dachs, J.; Benayas, J. Anthropogenic and biogenic hydrocarbons in soils and vegetation from the South Shetland Islands (Antarctica). *Sci. Total Environ.* **2016**, *569*–570, 1500–1509.
- (35) Degrendele, C.; Audy, O.; Hofman, J.; Kučerik, J.; Kukučka, P.; Mulder, M. D.; Přibylková, P.; Prokeš, R.; Šáňka, M.; Schaumann, G. E.; Lammel, G. Diurnal variations of air-soil exchange of semivolatile organic compounds (PAHs, PCBs, OCPs, and PBDEs) in a central European receptor area. *Environ. Sci. Technol.* **2016**, *50* (8), 4278–4288.
- (36) Simoneit, B. R.; Grimalt, J. O.; Wang, T. G.; Cox, R. E.; Hatcher, P. G.; Nissenbaum, A. Cyclic terpenoids of contemporary resinous plant detritus and of fossil woods, ambers and coals. *Org. Geochem.* **1986**, *10* (4–6), 877–889.
- (37) Qin, S.; Sun, Y.; Tang, Y.; Jin, K. Early diagenetic transformation of terpenoids from conifers in the aromatic hydrocarbon fraction: A long term, low temperature maturation experiment. *Org. Geochem.* **2012**, *53*, 99–108.
- (38) Macdonald, R.; Mackay, D.; Hickie, B. Contaminant amplification in the environment. *Environ. Sci. Technol.* **2002**, *36*, 456A–462A.
- (39) Bao, T.; Zhu, R.; Li, X.; Ye, W.; Cheng, X. Effects of multiple environmental variables on tundra ecosystem respiration in maritime Antarctica. *Sci. Rep.* **2018**, *8* (1), 12336.
- (40) Kukučka, P.; Lammel, G.; Dvorská, A.; Klánová, J.; Möller, A.; Fries, E. Contamination of Antarctic snow by polycyclic aromatic hydrocarbons dominated by combustion sources in the polar region. *Environ. Chem.* **2010**, *7*, 504.
- (41) Keyte, I. J.; Harrison, R. M.; Lammel, G. Chemical reactivity and long-range transport potential of polycyclic aromatic hydrocarbons — a review. *Chem. Soc. Rev.* **2013**, *42*, 9333–9391.
- (42) Stohl, A.; Sodemann, H. Characteristics of atmospheric transport into the Antarctic troposphere. *J. Geophys. Res.* **2010**, *115*, D02305.
- (43) Casal, P.; Zhang, Y.; Martin, J. W.; Pizarro, M.; Jiménez, B.; Dachs, J. Role of Snow Deposition of Perfluoroalkylated Substances at Coastal Livingston Island (Maritime Antarctica). *Environ. Sci. Technol.* **2017**, *51* (15), 8460–8470.
- (44) Jurado, E.; Jaward, F.; Lohmann, R.; Jones, K. C.; Simó, R.; Dachs, J. Wet deposition of persistent organic pollutants to the global oceans. *Environ. Sci. Technol.* **2005**, *39*, 2426–2435.
- (45) Bamford, H. A.; Poster, D. L.; Baker, J. E. Temperature dependence of Henry's law constants of thirteen polycyclic aromatic hydrocarbons between 4 and 31 °C. *Environ. Toxicol. Chem.* **1999**, *18* (9), 1905–1912.
- (46) Jurado, E.; Lohmann, R.; Meijer, S.; Jones, K. C.; Dachs, J. Latitudinal and seasonal capacity of the surface oceans as a reservoir of polychlorinated biphenyls. *Environ. Pollut.* **2004**, *128*, 149–162.
- (47) Dickhut, R. M.; Cincinelli, A.; Cochran, M.; Ducklow, H. W. Atmospheric concentrations and air–water flux of organochlorine pesticides along the Western Antarctic Peninsula. *Environ. Sci. Technol.* **2005**, *39* (2), 465–470.
- (48) Bigot, M.; Muir, D. C.; Hawker, D. W.; Cropp, R.; Dachs, J.; Teixeira, C. F.; Bengtson Nash, S. Air–seawater exchange of organochlorine pesticides in the southern ocean between Australia and Antarctica. *Environ. Sci. Technol.* **2016**, *50* (15), 8001–8009.

(49) Bigot, M.; Hawker, D. W.; Cropp, R.; Muir, D. C.; Jensen, B.; Bossi, R.; Bengtson Nash, S. M. Spring melt and the redistribution of organochlorine pesticides in the sea-ice environment: A comparative study between Arctic and Antarctic regions. *Environ. Sci. Technol.* **2017**, *51* (16), 8944–8952.

(50) Geisz, H. N.; Dickhut, R. M.; Cochran, M. A.; Fraser, W. R.; Ducklow, H. W. Melting glaciers: a probable source of DDT to the Antarctic marine ecosystem. *Environ. Sci. Technol.* **2008**, *42* (11), 3958–3962.

(51) Khairy, M. A.; Luek, J. L.; Dickhut, R.; Lohmann, R. Levels, sources and chemical fate of persistent organic pollutants in the atmosphere and snow along the western Antarctic Peninsula. *Environ. Pollut.* **2016**, *216*, 304–313.

(52) Maskey, S.; Geng, H.; Song, Y. C.; Hwang, H.; Yoon, Y. J.; Ahn, K. H.; Ro, C. U. Single-particle characterization of summertime antarctic aerosols collected at King George island using quantitative energy-dispersive electron probe X-ray microanalysis and attenuated total reflection Fourier transform-infrared imaging techniques. *Environ. Sci. Technol.* **2011**, *45* (15), 6275–6282.

(53) Haritash, A. K.; Kaushik, C. P. Biodegradation aspects of polycyclic aromatic hydrocarbons (PAHs): a review. *J. Hazard. Mater.* **2009**, *169* (1–3), 1–15.

(54) Goldberg, S. J.; Nelson, C. E.; Viviani, D. A.; Shulse, C. N.; Church, M. J. Cascading influence of inorganic nitrogen sources on DOM production, composition, lability and microbial community structure in the open ocean. *Environ. Microbiol.* **2017**, *19*, 3450–3464.

(55) Berrojalbiz, N.; Dachs, J.; Ojeda, M. J.; Valle, M. C.; Castro-Jimenez, J.; Wollgast, J.; Ghiani, M.; Hanke, G.; Zaldivar, J. M. Biogeochemical and physical controls on concentrations of polycyclic aromatic hydrocarbons in water and plankton of the Mediterranean and Black Seas. *Global Biogeochem. Cycles* **2011**, *25*, 1–14.

(56) Garneau, M. È.; Michel, C.; Meisterhans, G.; Fortin, N.; King, T. L.; Greer, C. W.; Lee, K. Hydrocarbon biodegradation by Arctic sea-ice and sub-ice microbial communities during microcosm experiments, Northwest Passage (Nunavut, Canada). *FEMS Microbiology Ecology* **2016**, *92* (10), fiv130.

(57) Vergeynst, L.; Wegeberg, S.; Aamand, J.; Lassen, P.; Gosewinkel, U.; Fritt-Rasmussen, J.; Gustavson, K.; Mosbech, A. Biodegradation of marine oil spills in the Arctic with a Greenland perspective. *Sci. Total Environ.* **2018**, *626*, 1243–1258.

(58) Okere, U. V.; Cabrerizo, A.; Dachs, J.; Jones, K. C.; Semple, K. T. Biodegradation of phenanthrene by indigenous microorganisms in soils from Livingstone Island, Antarctica. *FEMS Microbiol. Lett.* **2012**, *329* (1), 69–77.